Organic carbon decomposition rates with depth and contribution of inorganic carbon to CO 2 emissions under a Mediterranean agroforestry system

R. Cardinael, T. Chevallier, B. Guenet, Cyril Girardin, T. Cozzi, Valérie Pouteau, Claire Chenu

Organic carbon decomposition rates with depth and contribution of inorganic carbon to CO_2 emissions under a Mediterranean agroforestry system

R. CARDINAEL[a,b,c,d*], T. CHEVALLIER[a], B. GUENET[e], C. GIRARDIN[f], T. COZZI[b], V. POUTEAU[f], C. CHENU[b]

[a]Eco&Sols, IRD, CIRAD, INRA, Montpellier SupAgro, Univ Montpellier, Montpellier, France

[b]AgroParisTech, UMR Ecosys, Avenue Lucien Brétignières, 78850 Thiverval-Grignon, France

[c]CIRAD, UPR AIDA, F-34398 Montpellier, France (present address)

[d]AIDA, Univ Montpellier, CIRAD, Montpellier, France

[e]Laboratoire des Sciences du Climat et de l'Environnement, LSCE/IPSL, CEA-CNRS-UVSQ, Université Paris-Saclay, Gif-sur-Yvette, France

[f]INRA, UMR Ecosys, Avenue Lucien Brétignières, 78850 Thiverval-Grignon, France

*Corresponding author. E-mail address: remi.cardinael@cirad.fr

This article has been accepted for publication and undergone full peer review but has not been through the copyediting, typesetting, pagination and proofreading process which may lead to differences between this version and the Version of Record. Please cite this article as doi: 10.1111/ejss.12908

Summary

Agroforestry systems have been much studied for their potential to store soil organic carbon (SOC). However, few data are available on their specific impact on potential SOC mineralization, especially at depth in subsoils. Moreover, many soils of the world, especially in arid and semi-arid environments, also contain large stocks of soil inorganic carbon (SIC) as carbonates. Consequently, the organic carbon dynamics has been poorly investigated in these soils due to the complexity of measurements and of the processes involved. To assess mineralization rates of SOC with depth, we incubated soil samples coming from an 18-year-old agroforestry system (both tree row and alley) and an adjacent agricultural plot established on a calcareous soil in France. Soil samples were taken at four different depths: 0-10, 10-30, 70-100 and 160-180 cm. Total CO_2 emissions, the isotopic composition ($\delta^{13}C$, ‰) of the CO_2 and microbial biomass were measured. The SIC concentrations ranged from 48 to 63 g C kg^{-1} soil and the SOC concentrations ranged from 4 to 17 g C kg^{-1} soil. The contribution of SIC-derived CO_2 represented about 20% in the topsoil and 60% in the subsoil of the total soil CO_2 emissions. The microbial biomass and the SOC-derived CO_2 emissions were larger in the topsoil, but the decomposition rates (day^{-1}) remained stable with depth, suggesting that only the size of the labile carbon pool was modified with depth. Subsoil organic carbon seems to be as prone to decomposition as surface organic carbon. No difference in CO_2 emissions was found between the agroforestry and the control plot, except in the tree row at 0-10 cm. Our results

suggest that the measurement of soil respiration in calcareous soils could be overestimated if the isotopic signature of the CO_2 is not taken into account. It also advocates more in-depth studies on carbonate dissolution-precipitation processes and their impact on CO_2 emissions.

Keywords: Mediterranean, carbonates, soil respiration, ^{13}C natural abundance, microbial biomass, metabolic quotient, deep soil

Highlights

1) We measured SOC mineralisation and inorganic carbon contribution to CO_2 emissions in agroforestry

2) Subsoil organic carbon was as prone to decomposition as surface organic carbon

3) Inorganic carbon contribution to CO_2 emissions ranged from 20% to 60% depending on soil depth

4) Measurement of soil respiration in calcareous soils could be overestimated

Introduction

Agroforestry systems associate trees and crops or pastures within the same field (Nair, 1993). These systems usually provide enhanced ecosystem services compared to treeless farming systems (Torralba et al., 2016), especially in terms of soil organic carbon (SOC) storage (Cardinael et al., 2018a). This ecosystem service has been extensively studied in tropical

agroforestry systems (Albrecht & Kandji, 2003; Lorenz & Lal, 2014; Kim et al., 2016), but also more recently in temperate and Mediterranean agroforestry systems (Cardinael et al., 2015a, 2017, 2019; Pardon et al., 2017). Deep rooting of agroforestry trees (Mulia & Dupraz, 2006; Cardinael et al., 2015b) increase organic carbon inputs and could modify SOC dynamics in deep soil layers (Cardinael et al., 2018b). However, the measured SOC stocks in deep soil layers are not always significantly larger in agroforestry systems compared to treeless agricultural systems (Cardinael et al., 2015a; Upson et al., 2016).

The processes controlling SOC dynamics are still insufficiently understood, especially at depth (Salomé et al., 2010; Rumpel & Kögel-Knabner, 2011). Nevertheless, most studies have showed that SOC turnover was slower at depth (Mathieu et al., 2015; Tian et al., 2016; Balesdent et al., 2018). The proposed explanations are diverse: (i) deep SOC is depleted in energy-rich plant material (Fontaine et al., 2007); (ii) interactions between organic matter and minerals become the main factor of C stabilization with depth (Kleber et al., 2015; Mathieu et al., 2015); (iii) the SOC content decreases with depth with a spatial separation of SOC, microorganisms and extracellular enzyme activity which impedes microbial SOC mineralization (Rumpel & Kögel-Knabner, 2011); (iv) lower oxygen supply might limit decomposition (Keiluweit et al., 2016, 2017); (v) microbial biomass dramatically decreases with depth (Taylor et al., 2002; Fang & Moncrieff, 2005; Eilers et al., 2012); and (vi) the microbial populations in topsoil and subsoil have different metabolisms (Spohn et al., 2016). Even though mineralisation rates of SOC tend to decrease with soil depth, the decomposition per unit of C does not always depend on soil depth (e.g. Salomé et al., 2010). Microbial carbon

use efficiency may be similar in topsoil and subsoil (Spohn et al., 2016) and deep SOC can significantly contribute to SOC mineralization potential (Bounouara et al., 2017; Wordell-Dietrich et al., 2017). More studies are, thus, needed to estimate the processes of SOC mineralisation potentials in deep soil, especially under agroforestry system management where tree roots can provide C inputs (root mortality and root exudates) in deep soil horizons (Germon et al., 2016). Moreover, these estimations of SOC mineralisation potentials are essential for modelling purposes (Braakhekke et al., 2011, 2013; Guenet et al., 2013; Cardinael et al., 2018b).

Globally, arid and semiarid regions cover more than 30% of the Earth's land surface (Lal & Kimble, 2000; Romanyà & Rovira, 2011). Soils in these regions are usually calcareous and contain large amounts of inorganic carbon in the form of carbonates ($CaCO_3$), with a total inorganic carbon pool ranging from 750 to 950 PgC (Eswaran et al., 2000). Estimations of SOC mineralisation potentials are often based on laboratory soil incubations at optimal soil moisture and temperature conditions (Collins et al., 2000). The estimation of SOC mineralization rates in calcareous soils is complex because the presence of large amounts of soil inorganic carbon (SIC) may challenge the analysis of the carbon (C) fluxes from SOC mineralisation at the soil-air interface (Tamir et al., 2011, 2012; de Soto et al., 2017). As a consequence, little research on SOC dynamics has been carried out on these soils, and most studies (in particular C-cycle models) consider carbonates and SIC as a static C pool in soils, whereas the C flux from the inorganic C-cycle might be largely significant even at short timescales (Serrano-Ortiz et al.,

2009, 2010; Sanchez-Cañete et al., 2011), and are an important part of the global C cycle dynamics (Lal & Kimble, 2000).

The dynamics of SIC are related to the existence of carbonate dissolution and precipitation cycles in soil. These cycles are interrelated to biotic activities producing CO_2 which can be precipitated as carbonate (Gocke et al., 2011) and/or producing hydrogen ions or organic acids during biological pH-active reactions such as nitrification from decomposing organic matter, which may improve carbonate dissolution and stimulate CO_2 emissions from soils (Tamir et al., 2013; Chevallier et al., 2016; de Soto et al., 2017). The three main factors controlling dissolution and precipitation of carbonates as listed by Gocke et al., (2011) are: (1) CO_2 partial pressure in pore space, (2) pH of soil solution, and (3) mass flow of dissolved carbon species (H_2CO_3, HCO_3^-). Biological activities impact these three factors and thus may mobilize SIC to emit CO_2 or promote $CaCO_3$ precipitation by modifying the equilibrium between the different dissolved, gaseous and solid SIC species. In addition, SIC also impacts SOC mineralisation indirectly by its role on soil aggregate formation and stabilization, and then on SOC protection from mineralization (Clough & Skjemstad, 2000; Shang & Tiessen, 2003; Fernández-Ugalde et al., 2011, 2014; Virto et al., 2011). Using the difference in $\delta^{13}C$ signatures between SOC and SIC, empirical research based on natural isotopic ^{13}C tracing has been used to evaluate the contribution of SIC to the CO_2 emitted from soils (Stevenson & Verburg, 2006; Schindlbacher et al., 2015; Soper et al., 2017). In the published literature, the contribution of SIC to total CO_2 emissions ranges from 10% to 40% (Inglima et al., 2009) and up to 70% at high temperatures (Chevallier et al., 2016).

In this study, we compared the SOC dynamics in the soil profile of an agroforestry plot established 18 years ago on a calcareous soil compared to an adjacent agricultural plot on the same soil. We hypothesized that (1) SOC mineralisation potentials would decrease with increasing soil depth, in both the agricultural control plot and the agroforestry plot; (2) SOC mineralisation potentials would differ in the agroforestry plot compared to the agricultural plot due to different SOC inputs in amount and in quality; and (3) SIC would significantly contribute to total CO_2 emissions and differ between the soil samples depth.

The aims of this study were twofold: (i) assess SOC potential mineralisation as a function of soil depth in an agroforestry plot compared to an agricultural control plot (ii) estimate the contribution of SIC to CO_2 emissions at different depths.

Materials and methods

Site description

Soils were collected at an experimental site 15 km North of Montpellier, France (Longitude 04°01′ E, Latitude 43°43′ N, elevation 54 m a.s.l.). The climate is sub-humid Mediterranean with an average temperature of 15.4°C and an average annual rainfall of 873 mm (years 1995–2013). The soil is a silty and carbonated deep alluvial Fluvisol (IUSS Working Group WRB, 2007). Gravels > 2mm represented less than 1% of soil mass in the first 2 meters of soil (Cardinael et al., 2015a). The site comprises a silvoarable system, associating walnut (*Juglans regia* × *nigra* cv. NG23) trees and durum wheat (*Triticum turgidum* L. subsp. *durum* (Desf.) Husn.), and an adjacent agricultural control plot where only the annual crop is cultivated. Trees

were planted in 1995, in parallel tree rows (13 × 4 m spacing) and have a current density of 110 trees ha^{-1}. A spontaneous and herbaceous vegetation grows in the tree rows. The soil is plowed annually to 20 cm depth and the durum wheat is fertilized with 120 kg N ha^{-1} yr^{-1}.

As explained in Cardinael et al., (2015a), this experimental site was not designed as traditional agronomical experiments with blocks and replicates, but with two large adjacent plots within a same field. Soil texture was previously analyzed for 24 profiles down to 2 m soil depth, following a random sampling design within the two plots. Soil texture was very similar across the sampling points (Cardinael et al., 2015a). In addition, both plots had the same previous land use and management before the planting of the trees, and are at the same elevation.

Soil collection, carbon and isotopic analyses

In May 2013, 193 soil cores (pseudo-replicates) were collected down to 2 m depth in the control plot (n= 93), in the agroforestry alley (n=60) and in the tree row (n=40) using a motor-driven micro caterpillar driller (8.5-cm diameter) (Cardinael et al., 2015a). Soil cores were then cut into 10 layers, 0-10, 10-30, 30-50, 50-70, 70-100, 100-120, 120-140, 140-160, 160-180 and 180-200 cm.

A previous study at this site analyzed SOC fractions at four depths, 0-10, 10-30, 70-100 and 160-180 cm (Cardinael et al., 2015a); subsequently we decided to incubate soil from these same four depths in the present study as results of SOC fractionation could help interpreting the results of CO_2 emissions. The incubation, therefore, comprised four soil replicates per location (control, tree row, alley) and per depth (0-10, 10-30, 70-100 and 160-180 cm) (n=48). Soil samples were air-dried, sieved at 5 mm, and all roots were manually removed. Soil organic

carbon concentration was analyzed on sub-samples sieved at 2 mm with a CHN elemental analyzer (Carlo Erba NA 2000, Milan, Italy) after carbonates were removed by acid fumigation with HCl (37%) vapours for 8 h, following Harris et al., (2001). The isotopic composition ($\delta^{13}C - SOC$, ‰) of SOC was also determined on these carbonate-free samples using an Isotope Ratio Mass Spectrometer (GC-IRMS; Isochrom Optima, Micromass, North Carolina, USA) coupled with the CHN elemental analyzer.

The concentration and the isotopic composition of carbonates were also determined on each sub-sample. For this, soil samples were put in the oven at 550°C for 6 h to oxidize the organic matter (Dean, 1974). The organic matter free samples (10 mg) reacted with orthophosphoric acid (H_3PO_4, 105%) during 16 h at 25°C (Coplen et al., 1983) in a reaction vessel that had previously been purified of any gases with a vacuum pump and liquid nitrogen, and the CO_2 emitted by this reaction was analyzed to determine SIC content and its isotopic composition ($\delta^{13}C - SIC$, ‰). After the reaction, the CO_2 was expanded into an evacuation system, and then condensed into an U-trap with liquid nitrogen cooling (McCrea, 1950; Jones & Kaiteris, 1983; Mucciarone & Williams, 1990). The system was pumped to remove any residue of non-condensable gas. The amount of CO_2 emitted by the reaction with H_3PO_4 was measured with a manometer, and then transferred to a sample tube to measure its $\delta^{13}C - SIC$ by IRMS as above.

Laboratory incubations and soil respiration

Forty grams of 5 mm sieved soil was placed in 500-mL glass jars with Teflon® rubber stoppers crimped on with aluminium seals. Soil samples were moistened to reach field capacity, at pF

2.5. Immediately after adding the water, the glass jars were flushed with CO_2 free air (19% O_2, 81% N_2). Soils were then incubated at 20°C in the dark. The CO_2 concentration and the $\delta^{13}C$ of the CO_2 were measured after 1, 3, 7, 14, 21, 28, 35 and 44 days. The CO_2 concentration was determined with a micro GC (Agilent 3000A, Santa Clara, USA). The isotopic composition ($\delta^{13}C$, ‰) of the CO_2–C was determined using a GC (Hewlett-Packard 5890, San José, USA) coupled to an IRMS as above. Jars were aerated when necessary and flushed again to ensure that CO_2 concentrations did not exceed 10,000 ppm.

Isotopic calculations

The CO_2 concentration measured in each glass jar was assumed to be a mix of CO_2 originating from the mineralization of organic compounds and from the dissolution of carbonates:

$$CO_2 = SOC - CO_2 + SIC - CO_2 \qquad (1)$$

where CO_2 concentrations are expressed in ppm

Carbon isotope ratio is presented in δ notation, defined as follows:

$$\delta(‰) = \frac{R_{sample} - R_{PDB}}{R_{PDB}} \times 1000 \qquad (2)$$

where R_{sample} is the $^{13}C/^{12}C$ isotope ratio of the sample and R_{PDB} is the $^{13}C/^{12}C$ ratio of the international pee dee belemnite (PDB) standard (Coplen, 1995). The analytical precision of the $\delta^{13}C$ measurements was 0.1‰. We assumed that the carbonates in the soil solution were in isotopic equilibrium with the solid carbonates (Bertrand et al., 2007). We also neglected the isotopic fractionation between SIC and the SIC-derived CO_2 and between SOC and the SOC-derived CO_2. Although CO_2 emission from SIC is prone to induce isotopic fractionation at

various steps (carbonate dissolution, chemical equilibrium with HCO_3^- and dissolved CO_2, CO_2 transfer towards the atmosphere), previous studies expect that this kind of phenomenon would have a limited impact in short term incubation (Rovira & Vallejo, 2008; Chevallier et al., 2016). In the same way, isotopic fractionation during the mineralization of SOC, which has been reported of limited amplitude or not significant, was also neglected in the calculations, as in many isotopic studies on SOC mineralization (Bertrand et al., 2007; Boström et al., 2007).

The contribution of SIC-derived CO_2 (f_{SIC}) was estimated using a two-end member mixing model (Balesdent et al., 1987; Ramnarine et al., 2012):

$$\delta^{13}C - CO_2 \quad = f_{SIC} \times \delta^{13}C - SIC \quad + (1 - f_{SIC}) \times \delta^{13}C - SOC \qquad (3)$$

The equation can be rewritten as:

$$f_{SIC} = \frac{\delta^{13}C - CO_2 - \delta^{13}C - SOC}{\delta^{13}C - SIC - \delta^{13}C - SOC} \qquad (4)$$

with $\delta^{13}C - CO_2$ as the $\delta^{13}C$ of the total CO_2 emitted from soil sample, $\delta^{13}C - SOC$, the $\delta^{13}C$ of the SOC and $\delta^{13}C - SIC$, the $\delta^{13}C$ of the SIC of each soil samples.

If we assume that SIC emissions and SOC emissions are independent, the amount of CO_2 (µg C-CO_2 g^{-1} soil) derived from SOC respiration can be then calculated as follows:

$$SOC - CO_2 \quad = (1 - f_{SIC}) \times CO_2 \qquad (5)$$

The amount of CO_2 (µg C-CO_2 g^{-1} soil) derived from SIC is expressed as follows:

$$SIC - CO_2 \quad = f_{SIC} \times CO_2 \qquad (6)$$

SOC decomposition rates

Kinetic parameters are often derived from incubation experiments using models of different complexity to gain information about the carbon turnover. For a single-pool model, the total SOC is assumed to decompose with a certain turnover rate, whereas for the double-pool model the SOC is separated into two different compartments, i.e. into a labile pool with a short turnover time and into a non-labile or refractory pool with a longer turnover time (Qayyum et al., 2012). Given the short duration of the incubation in the present study (44 days), it was not possible to satisfactorily fit a two-pool model on the data, even using Bayesian calibration approaches. We, therefore, used a single-pool model, mainly corresponding to the decomposition of the labile pool during the duration of the experiment.

Here, we used a constrained fitting on % of total SOC mineralized data using a pool size (C_1) expressed in % of total SOC mineralized. At the end of the incubation (day 44), C_1 equals the total % of mineralized SOC (Weihermüller et al., 2018).

We used the following kinetic model to describe the data:

$$C_t = C_1 \times e^{-k_1 \times t} \qquad (8)$$

where C_t is the % SOC mineralized, C_1 is the total size of the labile carbon pool (%), k_1 is the corresponding decomposition rate (day^{-1}), and t is the duration of the incubation (day).

The mean residence time (MRT) was calculated from the decomposition rates by:

$$MRT = \frac{1}{k_1} \qquad (9)$$

In short-term incubations, the estimation of the decomposition rates can be uncertain, even for the labile pool. Several authors have proposed to use Bayesian calibration approaches to

analyze the real uncertainty and the identifiability of the parameter estimation (Scharnagl et al., 2010; Li et al., 2013; Schädel et al., 2013). We used a probabilistic inversion approach, using the *BayesianTools* R package (Hartig et al., 2018) and the *runMCMC* function to apply Markov chain Monte Carlo (MCMC) methods to our data. The prior probability distribution function (PDF) of the estimated parameters was specified as the uniform distributions over a set of specific intervals. The probabilistic inversion was performed using a Markov chain Monte Carlo algorithm (function *runMCMC*) to construct posterior probability density functions of parameters. The algorithm was run 20000 times until convergence. Convergence was tested using the Gelman–Rubin convergence diagnostic (function *gelmanDiagnostics*).

Microbial biomass and metabolic quotient

At the end of the incubations (day 44), microbial biomass carbon (MBC) was determined for each sample using 5 g of soil, and following the fumigation-extraction method described by Vance et al., (1987). The solution extracted with K_2SO_4 (5g/L) was analyzed with a TOC analyzer (TOC 505A, Shimadzu, Autosampler ASI-5000A, Tokyo, Japan). Microbial biomass carbon content was calculated as E_C/K_{EC}, where E_C is the difference between extracted organic C of fumigated and non-fumigated soils and K_{EC} = 0.45 (Wu et al., 1990; Jenkinson et al., 2004).

The metabolic quotient or specific respiration of the biomass (qCO_2) is the ratio of soil basal respiration to microbial biomass. The quotient qCO_2 is expressed in mg C-CO_2 µg C_{mic}^{-1} h^{-1} 10^{-4}. It indicates the ecophysiological status of soil microorganisms (Anderson & Domsch, 1985,

1993). For the calculation of the qCO_2, the hourly SOC-derived CO_2 (soil heterotrophic respiration) ($SOC - CO_2$ in mg C-CO_2 g^{-1} soil h^{-1}) was taken after soils had reached a relatively constant CO_2 production rate, between day 35 and day 44, just before the measurement of microbial biomass.

Statistical analyses

To test for general sampling location (tree row, alley, control) and depth effects on the different variables (Table S1), we performed a general linear mixed model (GLMM) analysis, with depth and sampling location as fixed factors and soil cores (pseudoreplicates) nested in the sampling location as a random factor to control for pseudoreplication and potential sampling location effects. Since samples from each soil core (four depths) were not independent from each other, we accounted for this correlation incorporating a symmetrical compound covariance matrix. For this analysis, we used all the collected samples per sampling location (N=3), soil cores (N=4) and depth (N=4), resulting in a total of 48 samples. Residuals were assessed for normality both visually using frequency distributions and Q-Q plots and statistically using Shapiro-Wilk tests, and data were log-transformed when necessary. The significance of the fixed factor was tested with a type-II analysis of variance and chi-square Wald tests (χ^2). Simple pair-wise comparisons between treatments were then performed on the GLMMs with Student's t-test.

All the statistical analyses were performed using R software version 3.1.1 (R Development Core Team, 2013), at a significance level of < 0.05. GLMMs were done using the *lmer* function

from the *lme4* package (Bates, 2010). Simple pair-wise comparisons were done using the *lsmeans* function from the *lsmeans* package (Lenth, 2016)

Results

Concentrations and $\delta^{13}C$ of soil organic and inorganic carbon

The ANOVA revealed that SOC concentrations were significantly dependent on sampling location, depth and on their interaction (Table S1). Soil organic carbon concentrations decreased with depth and were less than 10 mg C g^{-1} soil (i.e. < 1%) for all locations and depths, except in the tree row at 0-10 cm (Table 1). They were significantly larger in the tree row than in the alley (p-value < 0.001) and in the control plot (p-value < 0.001) at 0-10 cm depth. The same was found at 10-30 cm (p-value = 0.02 and 0.01, respectively). No significant difference between locations was found below 30 cm depth. The C/N ratio was significantly dependent on sampling location and on soil depth (Table S1).

Soil inorganic concentrations were very high and on average eight to ten times larger than SOC concentration (Table 1) and were significantly dependent on sampling location and on soil depth (Table S1).

Clay and silt content were similar at 0-10 cm and 10-30 cm and then increased with soil depth (Table 1).

The $\delta^{13}C - SOC$ was significantly dependent on soil depth and on the interaction between sampling location and soil depth (Table S1). At 0-10 cm, $\delta^{13}C - SOC$ was significantly less in the tree row (-27.57‰) than in the alley (-26.58‰) and in the control plot (-26.60‰) (p-values

< 0.001) (Table 2). For all sampling locations, the largest $\delta^{13}C - SOC$ was found at 70-100 cm (Table 2).

The $\delta^{13}C - SIC$ was significantly dependent on sampling location (p-value = 0.02) and soil depth (p-value = 0.04) (Table S1), but values remained very similar and were about -2 ‰ (Table 2). The $\delta^{13}C$ signature of SIC and SOC differed by more than -20 ‰.

Cumulated total, SOC- and SIC-derived CO_2 emissions from soils

The $\delta^{13}C$ signature of CO_2 emitted from soils differed from that of the SOC. The CO_2 emissions were ^{13}C-enriched by around 5‰ to 15‰ compared to the SOC and were therefore shifted towards the $\delta^{13}C$ signatures of SIC, especially at depth (Fig. 1). For a given soil sample, $\delta^{13}C$ signatures of evolved CO_2 did not vary much during the incubation period (± 2‰) (data not shown).

At the end of the incubation, the cumulated CO_2, $SOC - CO_2$ and $SIC - CO_2$ emissions were all significantly dependent on sampling location, on soil depth and on their interaction (Table S1). However, total CO_2, $SOC - CO_2$ and $SIC - CO_2$ emissions were only significantly higher in tree row than in the alley or in the control plot at 0-10 cm (p-values < 0.001) (Table 3). Below this topsoil layer, there was no significant difference between sampling locations.

In the alley and in the control plot, no significant difference was found between cumulated $SOC - CO_2$ emissions at 0-10 cm and at 10-30 cm (p-value = 0.54 and 0.14, respectively) (Table 3). However in the tree row, cumulated $SOC - CO_2$ emissions were significantly higher

at 0-10 cm than at 10-30 cm (p-value < 0.001). For the three sampling locations, cumulated $SOC - CO_2$emissions were significantly higher in the two topsoil layers than in the two subsoil layers.

Contribution of SIC and SOC to the emitted CO_2 from soils

Calculated contributions of $SIC - CO_2$ to total CO_2 emissions according to Eq. 4 and 6 were comprised between 15 and 30% in topsoil layers and between 50 and 70% in subsoil layers (Fig. 2). In topsoil layers, most of the total emitted CO_2 originated from SOC, while in deep soil layers it mainly originated from SIC (Fig. 2). In general, the relative contribution of $SIC - CO_2$ to total CO_2 emissions was slightly higher at the beginning of the incubation and decreased after one day of incubation to reach an equilibrium within one week (Fig. 2). We found an exponential relationship between the contribution of SIC to the total soil C and the contribution of $SIC - CO_2$ to the total CO_2 emissions with a coefficient of determination of 0.69 (Fig. 3A). Cumulative $SIC - CO_2$ emissions were also correlated to cumulative $SOC - CO_2$ emissions and a saturation model was significantly fitted (Fig. 3B).

Percentage of SOC mineralized and SOC decomposition rates

The percentage of initial SOC mineralized at the end of the incubation decreased with depth. At 0-10 cm, 2.94 ± 0.07 %, 1.66 ± 0.28 % and 1.92 ± 0.24 % of initial SOC were mineralized after 44 days of incubation, in the tree rows, alleys and in the control (Table 3, Fig. 4). At 160-180 cm, only 0.20% of SOC was mineralized whatever the location. No clear difference was observed depending on the sampling location, except at 0-10 cm in the tree row where a higher

proportion of total SOC was mineralized, and at 70-100 cm in the alley where this proportion was lower compared to other locations (Fig. 4).

The SOC decomposition rate k_1 and the mean residence time (*MRT*) were significantly dependent on soil depth (p-values = 0.003 and < 0.001, respectively) even if trends were not clear, but they were not significantly dependent on sampling location (Table S1). For a given depth, the SOC decomposition rate k_1 did not significantly change with sampling location. At 0-10 cm, k_1 was 0.059 day^{-1} in the tree row, 0.081 day^{-1} in the alley and 0.076 day^{-1} in the control, but no difference was found (Table 4).

Microbial biomass and qCO_2

At 70-100 cm and 160-180 cm, the MBC was below the detection threshold of the analyzer (Table 5). The ANOVA showed at MBC was significantly dependent on sampling location, on soil depth and on their interaction (Table S1). At 0-10 cm, the MBC was more than four times greater in the tree row than in the alley and in the control, and MBC contribution to SOC was also two times higher (Table 5). At 10-30 cm, there was no significant difference between the different locations. In the tree row, the MBC was significantly higher at 0-10 cm than at 10-30 cm (p-value < 0.001). The qCO_2 was neither significantly dependent on sampling location nor on soil depth (Table S1).

Discussion

Contribution of SIC-derived CO_2 to total emissions

Soil inorganic carbon contributed to the total CO_2 emissions from soil at each soil depth, each sampling location and during the whole period of soil incubation. The enrichment by 5 to 15‰ of ^{13}C of the total CO_2 emissions compared to the SOC can not only derive from the isotopic fractionation during the SOC mineralization (Schweizer et al., 1999). This increase in $\delta^{13}C$ of the CO_2 emissions cannot be explained without the contribution of an external C pool with high $\delta^{13}C$ and, hence, indicated a contribution of SIC to total CO_2 emissions (Stevenson & Verburg, 2006). This contribution was about 15 to 30% in the topsoil and quite close to the values encountered in literature for soil incubations in similar conditions to ours (Bertrand et al., 2007; Inglima et al., 2009; Chevallier et al., 2016). Even though SOC was the main contributor to the substantial evolved CO_2 in the topsoil (Fig. 2; Table 3), our results suggest that ignoring the contribution of SIC to soil respiration could lead to overestimations, especially in the subsoil where the contribution of $SIC - CO_2$ to total CO_2 emissions was greater than 60% (Ramnarine et al., 2012). However, the scale of this overestimation of soil respiration probably depends on the contribution of SIC to total soil C as shown in Fig. 3A. In our case, the SOC content was very low, and the amount of carbonates very high especially at depth.

The absolute amount of $SIC - CO_2$decreased with depth while the amount of SIC was similar in top and subsoil. Similarly, $SIC - CO_2$ emissions were larger at 0-10 cm in the tree rows than in the alley or in the control (Table 3), while there was no significant difference in SIC contents (Table 1). This seems to indicate that CO_2 emissions from SIC were linked to the SOC content and its mineralization. At 0-10 cm in the tree row, SOC concentration and microbial biomass were high. Moreover, particulate organic matter represents an important part of total SOC in

this layer (Cardinael et al., 2015a). These very labile OM soil fractions produce organic acids during decomposition (Adeleke et al., 2017), which could trigger carbonate dissolution. The high microbial biomass at 0-10 cm in the tree row leads to increased microbial respiration. This high production of CO_2 might destabilize the $CaCO_3/HCO_3^-/H_2CO_3/CO_2$ equilibrium and induce exchanges of C between SIC and SOC derived CO_2 (Tamir et al., 2013; Chevallier et al., 2017). The contribution of $SIC - CO_2$, or its apparent contribution, to total CO_2 emissions seemed to be partially controlled by the contribution of SIC content to total soil C, and by the amount of $SOC - CO_2$ (Fig. 3). As already pointed out by Chevallier et al., (2016, 2017), the assumption that $SOC - CO_2$ and $SIC - CO_2$ are independent is thus probably incorrect. The use of $\delta^{13}C$ analysis to determine the contribution of SIC and SOC to total CO_2 emissions from soil has been used widely but is still questionable in calcareous soils. Exchanges of C in the soil solution between C derived from SOC mineralisation and C derived from SIC dissolution might occur, especially in laboratory incubations with optimal soil moisture. Indeed, the CO_2 emitted by SOC can replace and displace SIC as carbonate (Lopez-Sangil et al., 2013), which could generate SIC-labeled CO_2 without a real contribution or losses of SIC to CO_2 (Rovira & Vallejo, 2008). Consequently, the CO_2 emissions would be labelled SIC but the $SIC - CO_2$ would be directly influenced by SOC. Due to the complexity and diversity of involved phenomena, such as C exchanges between SOC and SIC pools, but also possible isotopic fractionation between SOC or SIC and their respective CO_2 emissions (Skidmore et al. 2004), our data cannot disentangle the real implication of the SIC to measured CO_2 emissions, and the real contribution of carbonates to CO_2 emissions might be overestimated. Nevertheless, our data highlighted the need of additional information to unravel the mechanisms underlying the effect of SOC

mineralization on SIC dissolution and precipitation, and consequently on the measured $\delta^{13}C$-CO_2.

Subsoil OC is as prone to decomposition as surface OC

As expected, $SOC - CO_2$ emissions were larger in the topsoil than in the subsoil. However, the SOC decomposition rates were similar in the topsoil and in the subsoil, suggesting that deep SOC is as prone to decomposition as surface SOC under optimal incubation conditions (Stone & Plante, 2015). This, therefore, suggests that the size of the decomposing carbon pool was smaller in the subsoil, but its potential decomposition rate was not reduced (Salomé et al., 2010). Several incubation studies of different soil layers in the Mediterranean region also found that deep soil C was not more stable than topsoil C (Llorente & Turrion, 2010; Rovira et al., 2010; Bounouara et al., 2017). Given the short duration of the incubation (44 days), the carbon pool contributing to CO_2 emissions is likely to be a labile carbon pool, such as dissolved organic carbon or particulate organic carbon. The clay content of the two subsoil layers was almost two times higher than for the two topsoil layers (Table 1). The clay content is usually an important parameter to estimate the carbon stabilization potential of soils (Kleber et al., 2015). Unfortunately, the microbial biomass was too small to be quantified in the subsoil, but it was definitely very small as also shown by other authors (Fierer et al., 2003). As suggested by Wang et al., (2003), it, therefore, seems that under favourable temperature and moisture conditions and in short-term incubations, soil respiration is limited by the supply of biologically available substrate rather than by the clay content or the microbial biomass (Wang et al., 2003). In a Mediterranean context, Rovira & Vallejo, (1997) found that deep layers were more favourable

to microbial activity and litter decomposition than in upper layers in which drought and water availability were strong limiting factors. At our site, the same process might occur, potentially explaining why most of the additional SOC in the agroforestry plot was located in the topsoil despite important carbon inputs to deep soil layers (Cardinael et al., 2015a, 2018b).

No clear difference in SOC decomposition rate between the agroforestry and the control plots

The only significant difference between agroforestry and the control plot was observed at 0-10 cm where the SOC decomposition rate was lower in the tree row than in the alley or in the control (Table 4). Cardinael et al. (2015a) found that the important increase in SOC stocks in this soil layer was mainly due to particulate organic matter (POM) (50-200 and 200-2000 µm). In the present study, we also found that the $\delta^{13}C - SOC$ was significantly lower in this soil layer and that the C/N ratio was higher. We therefore suggest that the lower quality and the lignin content of the POMs (chemical recalcitrance) could explain the short-term slower potential decomposition rate at 0-10 cm in the tree rows (Schweizer et al., 1999; Thevenot et al., 2010). Another explanation (temperature and moisture being constant in this incubation) could be the lowest nutrient availability, tree rows receiving no mineral fertilizers, which might limit SOC decomposition (Averill & Waring, 2018). Cardinael et al., (2018b) found at the same site that, compared to the alleys, tree rows receive huge amounts of carbon, including tree root carbon, tree litterfall but also carbon from the understorey vegetation, potentially explaining a different chemical composition of the labile carbon pool. A parallel study on the same site on SOC mineralization from intact (3-5 mm) and crushed aggregates (< 200 µm) was performed as proposed by Chevallier et al., (2004), but results suggest that localization in millimetre size

soil aggregates is not the main mechanism explaining carbon stabilization at this site (unpublished data). More in-depth studies on SOC stabilization processes in agroforestry systems are required.

Conclusion

Our study revealed an important contribution of $SIC - CO_2$ in a calcareous soil potentially leading to an overestimation of soil respiration measured in arid and semi-arid regions, especially in deep soil layers. However, studies on fine-scale processes controlling the exchange of CO_2 emitted by SOC decomposition and CO_2 involved in dissolution-precipitation reactions are desperately missing to go beyond this result. Our study also confirmed previous findings showing that deep SOC can be as easily decomposed as surface SOC under optimal temperature and moisture conditions. No clear difference in SOC mineralization potentials was found between the agroforestry and the control plots. We conclude that deep SOC dynamics and stabilization processes should be more investigated in agroforestry and in carbonated soils given their potential impact on global warming.

Acknowledgments

This study was financed by the French Environment and Energy Management Agency (ADEME), following a call for proposals as part of the REACCTIF program (Research on Climate Change Mitigation in Agriculture and Forestry). This work was part of the funded project AGRIPSOL (Agroforestry for Soil Protection; 1260C0042) coordinated by Agroof.

Rémi Cardinael was supported both by ADEME and by La Fondation de France. The authors are grateful to Philippe Letourmy (CIRAD) for his help with the statistical analysis.

Data availability

The data that support the findings of this study are available from the corresponding author upon reasonable request.

References

Adeleke, R., Nwangburuka, C., & Oboirien, B. 2017. Origins, roles and fate of organic acids in soils: A review. *South African Journal of Botany* **108**, 393–406.

Albrecht, A., & Kandji, S.T. 2003. Carbon sequestration in tropical agroforestry systems. *Agriculture, Ecosystems and Environment* **99**, 15–27.

Anderson, T.H., & Domsch, K.H. 1985. Determination of ecophysiological maintenance carbon requirements of soil microorganisms in a dormant state. *Biology and Fertility of Soils* **1**, 81–89.

Anderson, T.H., & Domsch, K.H. 1993. The metabolic quotient for CO_2 (qCO_2) as a specific activity parameter to assess the effects of environmental conditions, such as pH, on the microbial biomass of forest soils. *Soil Biology and Biochemistry* **25**, 393–395.

Averill, C., & Waring, B. 2018. Nitrogen limitation of decomposition and decay: How can it occur? *Global Change Biology* **24**, 1417–1427.

Balesdent, J., Basile-Doelsch, I., Chadoeuf, J., Cornu, S., Derrien, D., Fekiacova, Z., & Hatté,

C. 2018. Atmosphere-soil carbon transfer as a function of soil depth. *Nature* **559**, 599–602.

Balesdent, J., Mariotti, A., & Guillet, B. 1987. Natural ^{13}C abundance as a tracer for studies of soil organic matter dynamics. *Soil Biology and Biochemistry* **19**, 25–30.

Bates, D.M. 2010. lme4: Mixed-effects modeling with R. , 145.

Bertrand, I., Delfosse, O., & Mary, B. 2007. Carbon and nitrogen mineralization in acidic, limed and calcareous agricultural soils: Apparent and actual effects. *Soil Biology and Biochemistry* **39**, 276–288.

Boström, B., Comstedt, D., & Ekblad, A. 2007. Isotope fractionation and ^{13}C enrichment in soil profiles during the decomposition of soil organic matter. *Oecologia* **153**, 89–98.

Bounouara, Z., Chevallier, T., Balesdent, J., Toucet, J., Sbih, M., Bernoux, M., Belaissaoui, N., Bouneb, O., & Bensaid, R. 2017. Variation in soil carbon stocks with depth along a toposequence in a sub-humid climate in North Africa (Skikda, Algeria). *Journal of Arid Environments* **141**, 25–33.

Braakhekke, M.C., Beer, C., Hoosbeek, M.R., Reichstein, M., Kruijt, B., Schrumpf, M., & Kabat, P. 2011. Somprof: A vertically explicit soil organic matter model. *Ecological Modelling* **222**, 1712–1730.

Braakhekke, M.C., Wutzler, T., Beer, C., Kattge, J., Schrumpf, M., Ahrens, B., Schöning, I., Hoosbeek, M.R., Kruijt, B., Kabat, P., & Reichstein, M. 2013. Modeling the vertical soil organic matter profile using Bayesian parameter estimation. *Biogeosciences* **10**, 399–420.

Cardinael, R., Chevallier, T., Barthès, B.G., Saby, N.P.A., Parent, T., Dupraz, C., Bernoux, M.,

& Chenu, C. 2015a. Impact of alley cropping agroforestry on stocks, forms and spatial distribution of soil organic carbon - A case study in a Mediterranean context. *Geoderma* **259**–**260**, 288–299.

Cardinael, R., Mao, Z., Prieto, I., Stokes, A., Dupraz, C., Kim, J.H., & Jourdan, C. 2015b. Competition with winter crops induces deeper rooting of walnut trees in a Mediterranean alley cropping agroforestry system. *Plant and Soil* **391**, 219–235.

Cardinael, R., Chevallier, T., Cambou, A., Béral, C., Barthès, B.G., Dupraz, C., Durand, C., Kouakoua, E., & Chenu, C. 2017. Increased soil organic carbon stocks under agroforestry: A survey of six different sites in France. *Agriculture, Ecosystems and Environment* **236**, 243–255.

Cardinael, R., Umulisa, V., Toudert, A., Olivier, A., Bockel, L., & Bernoux, M. 2018a. Revisiting IPCC Tier 1 coefficients for soil organic and biomass carbon storage in agroforestry systems. *Environmental Research Letters* **13**, 1–20.

Cardinael, R., Guenet, B., Chevallier, T., Dupraz, C., Cozzi, T., & Chenu, C. 2018b. High organic inputs explain shallow and deep SOC storage in a long-term agroforestry system - Combining experimental and modeling approaches. *Biogeosciences* **15**, 297–317.

Cardinael, R., Hoeffner, K., Chenu, C., Chevallier, T., Béral, C., Dewisme, A., & Cluzeau, D. 2019. Spatial variation of earthworm communities and soil organic carbon in temperate agroforestry. *Biology and Fertility of Soils* **55**, 171–183.

Chevallier, T., Blanchart, E., Albrecht, A., & Feller, C. 2004. The physical protection of soil organic carbon in aggregates: A mechanism of carbon storage in a Vertisol under pasture

and market gardening (Martinique, West Indies). *Agriculture, Ecosystems and Environment* **103**, 375–387.

Chevallier, T., Cournac, L., Bernoux, M., Cardinael, R., Cozzi, T., Girardin, C., & Chenu, C. 2017. Soil inorganic carbon and climate change in drylands? An emerging issue? *In* Global Symposium on Soil Organic Carbon (GSOC17). FAO, Rome, Italie.

Chevallier, T., Cournac, L., Hamdi, S., Gallali, T., & Bernoux, M. 2016. Temperature dependence of CO_2 emissions rates and isotopic signature from a calcareous soil. *Journal of Arid Environments* **135**, 132–139.

Clough, A., & Skjemstad, J.O. 2000. Physical and chemical protection of soil organic carbon in three agricultural soils with different contents of calcium carbonate. *Australian Journal of Soil Research* **38**, 1005–1016.

Collins, H.P., Elliott, E.T., Paustian, K., Bundy, L.G., Dick, W.A., Huggins, D.R., Smucker, A.J.M., & Paul, E.A. 2000. Soil carbon pools and fluxes in long-term Corn Belt agroecosystems. *Soil Biology and Biochemistry* **32**, 157–168.

Coplen, T.B. 1995. New IUPAC guidelines for the reporting of stable hydrogen, carbon, and oxygen isotope-ratio data. *Journal of Research of the National Institute of Standards and Technology* **100**, 285.

Coplen, T.B., Kendall, C., & Hopple, J. 1983. Comparison of stable isotope reference samples. *Nature* **21**, 28–30.

Dean, W.E. 1974. Determination of carbonate and organic matter in calcareous sediments and sedimentary rocks by loss on ignition; comparison with other methods. *Journal of*

Sedimentary Research **44**, 242–248.

Eilers, K.G., Debenport, S., Anderson, S., & Fierer, N. 2012. Digging deeper to find unique microbial communities: The strong effect of depth on the structure of bacterial and archaeal communities in soil. *Soil Biology and Biochemistry* **50**, 58–65.

Eswaran, H., Reich, P.F., Kimble, J.M., Beinroth, F.H., Padmanabhan, E., & Moncharoen, P. 2000. Global carbon sinks. p. 15–26. *In* Lal, R., Kimble, J.M., Eswaran, H., Stewart, B.A. (eds.), Global Climate Change and Pedogenic Carbonates. CRC Press, Boca Raton, FL.

Fang, C., & Moncrieff, J.B. 2005. The variation of soil microbial respiration with depth in relation to soil carbon composition. *Plant and Soil* **268**, 243–253.

Fernández-Ugalde, O., Virto, I., Barré, P., Apesteguía, M., Enrique, A., Imaz, M.J., & Bescansa, P. 2014. Mechanisms of macroaggregate stabilisation by carbonates: Implications for organic matter protection in semi-arid calcareous soils. *Soil Research* **52**, 180–192.

Fernández-Ugalde, O., Virto, I., Barré, P., Gartzia-Bengoetxea, N., Enrique, A., Imaz, M.J., & Bescansa, P. 2011. Effect of carbonates on the hierarchical model of aggregation in calcareous semi-arid Mediterranean soils. *Geoderma* **164**, 203–214.

Fierer, N., Allen, A.S., Schimel, J.P., & Holden, P.A. 2003. Controls on microbial CO_2 production: A comparison of surface and subsurface soil horizons. *Global Change Biology* **9**, 1322–1332.

Fontaine, S., Barot, S., Barré, P., Bdioui, N., Mary, B., & Rumpel, C. 2007. Stability of organic carbon in deep soil layers controlled by fresh carbon supply. *Nature* **450**, 277–280.

Germon, A., Cardinael, R., Prieto, I., Mao, Z., Kim, J., Stokes, A., Dupraz, C., Laclau, J.-P., & Jourdan, C. 2016. Unexpected phenology and lifespan of shallow and deep fine roots of walnut trees grown in a silvoarable Mediterranean agroforestry system. *Plant and Soil* **401**, 409–426.

Gocke, M., Pustovoytov, K., & Kuzyakov, Y. 2011. Carbonate recrystallization in root-free soil and rhizosphere of Triticum aestivum and Lolium perenne estimated by ^{14}C labeling. *Biogeochemistry* **103**, 209–222.

Guenet, B., Eglin, T., Vasilyeva, N., Peylin, P., Ciais, P., & Chenu, C. 2013. The relative importance of decomposition and transport mechanisms in accounting for soil organic carbon profiles. *Biogeosciences* **10**, 2379–2392.

Harris, D., Horwath, W.R., & van Kessel, C. 2001. Acid fumigation of soils to remove carbonates priori to total organic carbon or carbon-13 isotopic analysis. *Soil Science Society of America Journal* **65**, 1853–1856.

Hartig, F., Minunno, F., & Paul, S. 2018. BayesianTools: General-Purpose MCMC and SMC Samplers and Tools for Bayesian Statistics. R package version 0.1.4. https://CRAN.R-project.org/package=BayesianTools, 71p.

Inglima, I., Alberti, G., Bertolini, T., Vaccari, F.P., Gioli, B., Miglietta, F., Cotrufo, M.F., & Peressotti, A. 2009. Precipitation pulses enhance respiration of Mediterranean ecosystems: The balance between organic and inorganic components of increased soil CO_2 efflux. *Global Change Biology* **15**, 1289–1301.

IUSS Working Group WRB. 2007. World Reference Base for Soil Resources 2006, first update

2007. World Soil Resources Reports No. 103. FAO, Rome.

Jenkinson, D.S., Brookes, P.C., & Powlson, D.S. 2004. Measuring soil microbial biomass. *Soil Biology and Biochemistry* **36**, 5–7.

Jones, G.A., & Kaiteris, P. 1983. A vacuum-gasometric technique for rapid and precise analysis of calcium carbonate in sediments and soils. *Journal of Sedimentary Petrology* **2**, 655–660.

Keiluweit, M., Nico, P.S., Kleber, M., & Fendorf, S. 2016. Are oxygen limitations under recognized regulators of organic carbon turnover in upland soils? *Biogeochemistry* **127**, 157–171.

Keiluweit, M., Wanzek, T., Kleber, M., Nico, P., & Fendorf, S. 2017. Anaerobic microsites have an unaccounted role in soil carbon stabilization. *Nature Communications* **8**, 1–8.

Kim, D.G., Kirschbaum, M.U.F., & Beedy, T.L. 2016. Carbon sequestration and net emissions of CH_4 and N_2O under agroforestry: Synthesizing available data and suggestions for future studies. *Agriculture, Ecosystems and Environment* **226**, 65–78.

Kleber, M., Eusterhues, K., Keiluweit, M., Mikutta, C., Mikutta, R., & Nico, P.S. 2015. Mineral-Organic Associations: Formation, Properties, and Relevance in Soil Environments. Elsevier Ltd.

Lal, R., & Kimble, J.M. 2000. Pedogenic carbonates and the global carbon cycle. p. 1–14. *In* Lal, R., Kimble, J.M., Eswaran, H., Stewart, B.A. (eds.), Global Climate Change and Pedogenic Carbonates. CRC Press, USA.

Lenth, R. V. 2016. Least-Squares Means: The *R* Package **lsmeans**. *Journal of Statistical*

Software **69**.

Li, D., Schädel, C., Haddix, M.L., Paul, E.A., Conant, R., Li, J., Zhou, J., & Luo, Y. 2013. Differential responses of soil organic carbon fractions to warming: Results from an analysis with data assimilation. *Soil Biology and Biochemistry* **67**, 24–30.

Llorente, M., & Turrion, M.B. 2010. Microbiological parameters as indicators of soil organic carbon dynamics in relation to different land use management. *European Journal of Forest Research* **129**, 73–81.

Lopez-Sangil, L., Rovira, P., & Casals, P. 2013. Decay and vertical reallocation of organic C, and its incorporation into carbonates, in agricultural soil horizons at two different depths and rewetting frequencies. *Soil Biology and Biochemistry* **61**, 33–44.

Lorenz, K., & Lal, R. 2014. Soil organic carbon sequestration in agroforestry systems. A review. *Agronomy for Sustainable Development* **34**, 443–454.

Mathieu, J.A., Hatté, C., Balesdent, J., & Parent, É. 2015. Deep soil carbon dynamics are driven more by soil type than by climate: A worldwide meta-analysis of radiocarbon profiles. *Global Change Biology* **21**, 4278–4292.

McCrea, J.M. 1950. On the isotopic chemistry of carbonates and a paleotemperature scale. *The Journal of Chemical Physics* **18**, 849–857.

Mucciarone, D.A., & Williams, D.F. 1990. Stable isotope analyses of carbonates complicated by nitrogen contamination: a Delaware basin example. *Journal of Sedimentary Petrology* **60**, 608–614.

Mulia, R., & Dupraz, C. 2006. Unusual fine root distributions of two deciduous tree species in

southern France: What consequences for modelling of tree root dynamics? *Plant and Soil* **281**, 71–85.

Nair, P.K.R. 1993. An introduction to agroforestry. Kluwer Academic Publishers, Dordrecht, The Netherlands.

Pardon, P., Reubens, B., Reheul, D., Mertens, J., De Frenne, P., Coussement, T., Janssens, P., & Verheyen, K. 2017. Trees increase soil organic carbon and nutrient availability in temperate agroforestry systems. *Agriculture, Ecosystems and Environment* **247**, 98–111.

Qayyum, M.F., Steffens, D., Reisenauer, H.P., & Schubert, S. 2012. Kinetics of Carbon Mineralization of Biochars Compared with Wheat Straw in Three Soils. *Journal of Environment Quality* **41**, 1210–1220.

R Development Core Team. 2013. R: A language and environment for statistical computing.

Ramnarine, R., Wagner-Riddle, C., Dunfield, K.E., & Voroney, R.P. 2012. Contributions of carbonates to soil CO_2 emissions. *Canadian Journal of Soil Science* **92**, 599–607.

Romanyà, J., & Rovira, P. 2011. An appraisal of soil organic C content in Mediterranean agricultural soils. *Soil Use and Management* **27**, 321–332.

Rovira, P., Jorba, M., & Romanyà, J. 2010. Active and passive organic matter fractions in Mediterranean forest soils. *Biology and Fertility of Soils* **46**, 355–369.

Rovira, P., & Vallejo, V.R. 1997. Organic carbon and nitrogen mineralization under Mediterranean climatic conditions: The effects of incubation depth. *Soil Biology and Biochemistry* **29**, 1509–1520.

Rovira, P., & Vallejo, V.R. 2008. Changes in $\delta^{13}C$ composition of soil carbonates driven by

organic matter decomposition in a Mediterranean climate: A field incubation experiment. *Geoderma* **144**, 517–534.

Rumpel, C., & Kögel-Knabner, I. 2011. Deep soil organic matter - a key but poorly understood component of terrestrial C cycle. *Plant and Soil* **338**, 143–158.

Salomé, C., Nunan, N., Pouteau, V., Lerch, T.Z., & Chenu, C. 2010. Carbon dynamics in topsoil and in subsoil may be controlled by different regulatory mechanisms. *Global Change Biology* **16**, 416–426.

Sanchez-Cañete, E.P., Serrano-Ortiz, P., Kowalski, A.S., Oyonarte, C., & Domingo, F. 2011. Subterranean CO_2 ventilation and its role in the net ecosystem carbon balance of a karstic shrubland. *Geophysical Research Letters* **38**.

Schädel, C., Luo, Y., David Evans, R., Fei, S., & Schaeffer, S.M. 2013. Separating soil CO_2 efflux into C-pool-specific decay rates via inverse analysis of soil incubation data. *Oecologia* **171**, 721–732.

Scharnagl, B., Vrugt, J.A., Vereecken, H., & Herbst, M. 2010. Information content of incubation experiments for inverse estimation of pools in the Rothamsted carbon model: A Bayesian perspective. *Biogeosciences* **7**, 763–776.

Schindlbacher, A., Borken, W., Djukic, I., Brandstätter, C., Spötl, C., & Wanek, W. 2015. Contribution of carbonate weathering to the CO_2 efflux from temperate forest soils. *Biogeochemistry* **124**, 273–290.

Schweizer, M., Fear, J., & Cadisch, G. 1999. Isotopic (^{13}C) fractionation during plant residue decomposition and its implications for soil organic matter studies. *Rapid Communications*

in Mass Spectrometry **13**, 1284–1290.

Serrano-Ortiz, P., Domingo, F., Cazorla, A., Were, A., Cuezva, S., Villagarcía, L., Alados-Arboledas, L., & Kowalski, A.S. 2009. Interannual CO_2 exchange of a sparse Mediterranean shrubland on a carbonaceous substrate. *Journal of Geophysical Research: Biogeosciences* **114**, 1–11.

Serrano-Ortiz, P., Roland, M., Sanchez-Moral, S., Janssens, I.A., Domingo, F., Goddéris, Y., & Kowalski, A.S. 2010. Hidden, abiotic CO_2 flows and gaseous reservoirs in the terrestrial carbon cycle: Review and perspectives. *Agricultural and Forest Meteorology* **150**, 321–329.

Shang, C., & Tiessen, H. 2003. Soil organic C sequestration and stabilization in karstic soils of Yucatan. *Biogeochemistry* **62**, 177–196.

Soper, F.M., McCalley, C.K., Sparks, K., & Sparks, J.P. 2017. Soil carbon dioxide emissions from the Mojave desert: Isotopic evidence for a carbonate source. *Geophysical Research Letters* **44**, 245–251.

de Soto, I.S., Virto, I., Barré, P., Fernández-Ugalde, O., Antón, R., Martínez, I., Chaduteau, C., Enrique, A., & Bescansa, P. 2017. A model for field-based evidences of the impact of irrigation on carbonates in the tilled layer of semi-arid Mediterranean soils. *Geoderma* **297**, 48–60.

Spohn, M., Klaus, K., Wanek, W., & Richter, A. 2016. Microbial carbon use efficiency and biomass turnover times depending on soil depth - Implications for carbon cycling. *Soil Biology and Biochemistry* **96**, 74–81.

Stevenson, B.A., & Verburg, P.S.J. 2006. Effluxed CO_2-^{13}C from sterilized and unsterilized treatments of a calcareous soil. *Soil Biology and Biochemistry* **38**, 1727–1733.

Stone, M.M., & Plante, A.F. 2015. Relating the biological stability of soil organic matter to energy availability in deep tropical soil profiles. *Soil Biology and Biochemistry* **89**, 162–171.

Tamir, G., Shenker, M., Heller, H., Bloom, P.R., Fine, P., & Bar-Tal, A. 2011. Can Soil Carbonate Dissolution Lead to Overestimation of Soil Respiration? *Soil Science Society of America Journal* **75**, 1414–1422.

Tamir, G., Shenker, M., Heller, H., Bloom, P.R., Fine, P., & Bar-Tal, A. 2012. Dissolution and Re-crystallization Processes of Active Calcium Carbonate in Soil Developed on Tufa. *Soil Science Society of America Journal* **76**, 1606–1613.

Tamir, G., Shenker, M., Heller, H., Bloom, P.R., Fine, P., & Bar-Tal, A. 2013. Organic N mineralization and transformations in soils treated with animal waste in relation to carbonate dissolution and precipitation. *Geoderma* **209**–**210**, 50–56.

Taylor, J.P., Wilson, B., Mills, M.S., & Burns, R.G. 2002. Comparison of microbial numbers and enzymatic activities in surface soils and subsoils using various techniques. *Soil Biology and Biochemistry* **34**, 387–401.

Thevenot, M., Dignac, M.F., & Rumpel, C. 2010. Fate of lignins in soils: A review. *Soil Biology and Biochemistry* **42**, 1200–1211.

Tian, Q., Yang, X., Wang, X., Liao, C., Li, Q., Wang, M., Wu, Y., & Liu, F. 2016. Microbial community mediated response of organic carbon mineralization to labile carbon and

nitrogen addition in topsoil and subsoil. *Biogeochemistry* **128**, 125–139.

Torralba, M., Fagerholm, N., Burgess, P.J., Moreno, G., & Plieninger, T. 2016. Do European agroforestry systems enhance biodiversity and ecosystem services? A meta-analysis. *Agriculture, Ecosystems and Environment* **230**, 150–161.

Upson, M.A., Burgess, P.J., & Morison, J.I.L. 2016. Soil carbon changes after establishing woodland and agroforestry trees in a grazed pasture. *Geoderma* **283**, 10–20.

Vance, E.D., Brookes, P.C., & Jenkinson, D.S. 1987. An extraction method for measuring soil microbial biomass C. *Soil Biology and Biochemistry* **19**, 703–707.

Virto, I., Gartzia-Bengoetxea, N., & Fernández-Ugalde, O. 2011. Role of Organic Matter and Carbonates in Soil Aggregation Estimated Using Laser Diffractometry. *Pedosphere* **21**, 566–572.

Wang, W.J., Dalal, R.C., Moody, P.W., & Smith, C.J. 2003. Relationships of soil respiration to microbial biomass, substrate availability and clay content. *Soil Biology and Biochemistry* **35**, 273–284.

Weihermüller, L., Neuser, A., Herbst, M., & Vereecken, H. 2018. Problems associated to kinetic fitting of incubation data. *Soil Biology and Biochemistry* **120**, 260–271.

Wordell-Dietrich, P., Don, A., & Helfrich, M. 2017. Controlling factors for the stability of subsoil carbon in a Dystric Cambisol. *Geoderma* **304**, 40–48.

Wu, J., Joergensen, R.G., Pommerening, B., Chaussod, R., & Brookes, P.C. 1990. Measurement of soil microbial biomass C by fumigation-extraction-an automated procedure. *Soil Biology and Biochemistry* **22**, 1167–1169.

TABLES

Table 1 Soil characteristics. SOC: soil organic carbon; SIC: soil inorganic carbon. The carbon to nitrogen (C/N) ratio represents the C/N ratio of soil organic matter. N=4 for each soil depth and sampling location. Associated errors are standard errors.

Depth (cm)	SOC concentration (mg C g^{-1} soil)			SIC concentration (mg C g^{-1} soil)			C/N			Soil texture (g kg^{-1} soil) clay/silt/sand
	Control	Alley	Tree row	Control	Alley	Tree row	Control	Alley	Tree row	
0-10	7.4 ± 0.4	8.1 ± 0.5	16.9 ± 2.3	61.6 ± 0.9	54.9 ± 2.3	58.4 ± 2.8	9.5 ± 0.1	9.2 ± 0.1	9.9 ± 0.3	188/419/393
10-30	7.6 ± 0.1	8.1 ± 0.5	8.5 ± 0.6	62.3 ± 1.5	62.9 ± 3.7	58.8 ± 2.0	9.6 ± 0.2	9.4 ± 0.4	9.0 ± 0.2	180/409/411
70-100	5.3 ± 0.3	5.3 ± 0.1	5.1 ± 0.3	56.0 ± 2.7	48.0 ± 1.2	50.1 ± 1.9	8.2 ± 0.1	7.6 ± 0.3	7.4 ± 0.2	295/545/160
160-180	5.0 ± 0.5	4.8 ± 0.4	4.3 ± 0.4	52.5 ± 1.4	48.7 ± 1.7	52.5 ± 2.1	8.5 ± 0.1	7.6 ± 0.3	7.4 ± 0.4	334/577/89

Table 2 $\delta^{13}C$ (‰) values of soil organic carbon (SOC) and soil inorganic carbon (SIC). N=4 for each soil depth and sampling location. Associated errors are standard errors.

Depth (cm)	$\delta^{13}C - SOC$ (‰)			$\delta^{13}C - SIC$ (‰)		
	Control	Alley	Tree row	Control	Alley	Tree row
0-10	-26.60 ± 0.09	-26.58 ± 0.13	-27.57 ± 0.05	-1.78 ± 0.19	-2.00 ± 0.20	-2.09 ± 0.25
10-30	-26.61 ± 0.02	-26.57 ± 0.08	-26.47 ± 0.04	-1.71 ± 0.10	-1.76 ± 0.10	-2.35 ± 0.18
70-100	-25.10 ± 0.09	-25.25 ± 0.12	-24.92 ± 0.03	-2.05 ± 0.20	-2.34 ± 0.08	-2.16 ± 0.08
160-180	-25.76 ± 0.13	-25.83 ± 0.06	-25.70 ± 0.12	-1.83 ± 0.08	-1.76 ± 0.17	-1.94 ± 0.11

Table 3 SOC-derived CO_2 ($SOC - CO_2$), SIC-derived CO_2 ($SIC - CO_2$), and total cumulated CO_2 (CO_2) emissions after 44 days of incubations. N=4 for each soil depth and sampling location. Values in brackets represent the total percentage of SOC lost through soil respiration at the end of the incubation. Associated errors are standard errors. Significantly (p-value < 0.05) different values between sampling locations per soil depth are followed by different lowercase letters. Significantly (p-value < 0.05) different values between soil depths per sampling location are followed by different uppercase letters.

Depth (cm)	$SOC - CO_2$ (µg C g^{-1} soil)			$SIC - CO_2$ (µg C g^{-1} soil)			CO_2 (µg C g^{-1} soil)		
	Control	Alley	Tree row	Control	Alley	Tree row	Control	Alley	Tree row
0-10	144 ± 23 (1.92)	137 ± 33 (1.66)	497 ± 73 (2.94)	48 ± 4	45 ± 3	71 ± 2	192 ± 26	183 ± 35	569 ± 75
10-30	95 ± 5 (1.25)	119 ± 25 (1.44)	121 ± 12 (1.41)	39 ± 2	44 ± 3	42 ± 1	133 ± 7	163 ± 28	163 ± 12
70-100	17 ± 3 (0.32)	12 ± 1 (0.23)	17 ± 2 (0.33)	21 ± 1	19 ± 1	21 ± 2	38 ± 4	31 ± 1	38 ± 5
160-180	8 ± 0 (0.17)	9 ± 0 (0.21)	8 ± 1 (0.20)	14 ± 1	15 ± 1	13 ± 1	22 ± 1	24 ± 1	21 ± 2

Table 4 SOC decomposition rates (k_1) and mean residence time (*MRT*) of the labile carbon pool. The prior value was set for the estimation of k_1. Associated errors represent standard errors (N = 4).

Depth (cm)	Location	*Prior*	k_1 (day^{-1})	MRT (day)
0-10	Tree row	0.05 (0-2)	0.059 ± 0.002	16.99 ± 0.59
	Alley	0.05 (0-2)	0.081 ± 0.007	12.62 ± 1.13
	Control	0.05 (0-2)	0.076 ± 0.003	13.25 ± 0.47
10-30	Tree row	0.05 (0-2)	0.069 ± 0.004	14.55 ± 0.71
	Alley	0.05 (0-2)	0.068 ± 0.005	15.09 ± 1.17
	Control	0.05 (0-2)	0.064 ± 0.002	15.66 ± 0.60
70-100	Tree row	0.05 (0-2)	0.092 ± 0.007	11.08 ± 0.83
	Alley	0.05 (0-2)	0.095 ± 0.027	12.72 ± 2.52
	Control	0.05 (0-2)	0.086 ± 0.015	12.89 ± 2.37
160-180	Tree row	0.05 (0-2)	0.061 ± 0.003	16.50 ± 1.04
	Alley	0.05 (0-2)	0.061 ± 0.000	16.39 ± 0.00
	Control	0.05 (0-2)	0.057 ± 0.005	18.15 ± 2.11

Table 5 Soil microbial biomass carbon (MBC) and metabolic quotient. N=4 for each soil depth and sampling location. Associated errors are standard errors. Values in brackets represent the contribution of microbial biomass C to SOC (%). n.d. not determined as Microbial biomass-C was too low to be detectable.

Depth (cm)	Location	Microbial biomass-C ($\mu g\ C_{mic}\ g^{-1}$ soil)	*qCO₂* ($mg\ C\text{-}CO_2\ \mu g\ C_{mic}^{-1}\ h^{-1} * 10^{-4}$)
	Tree row	322.77 ± 64.63 (1.91)	8.14 ± 1.16

0-10	Alley	75.57 ± 15.06 (0.93)	9.07 ± 3.88
	Control	68.65 ± 10.58 (0.93)	8.56 ± 0.60
	Tree row	85.93 ± 14.67 (1.01)	7.88 ± 0.80
10-30	Alley	86.64 ± 16.96 (1.07)	7.53 ± 1.03
	Control	96.28 ± 12.51 (1.27)	5.49 ± 0.36
70-100	All	n.d.	n.d.
160-180	All	n.d.	n.d.

FIGURES

Figure 1 $\delta^{13}C$ (‰) profile of soil organic carbon (SOC), of soil inorganic carbon (SIC) and of the CO_2 emitted from the control, alley and the tree row soil samples between days 35 and 44 of incubation. Error bars are standard errors.

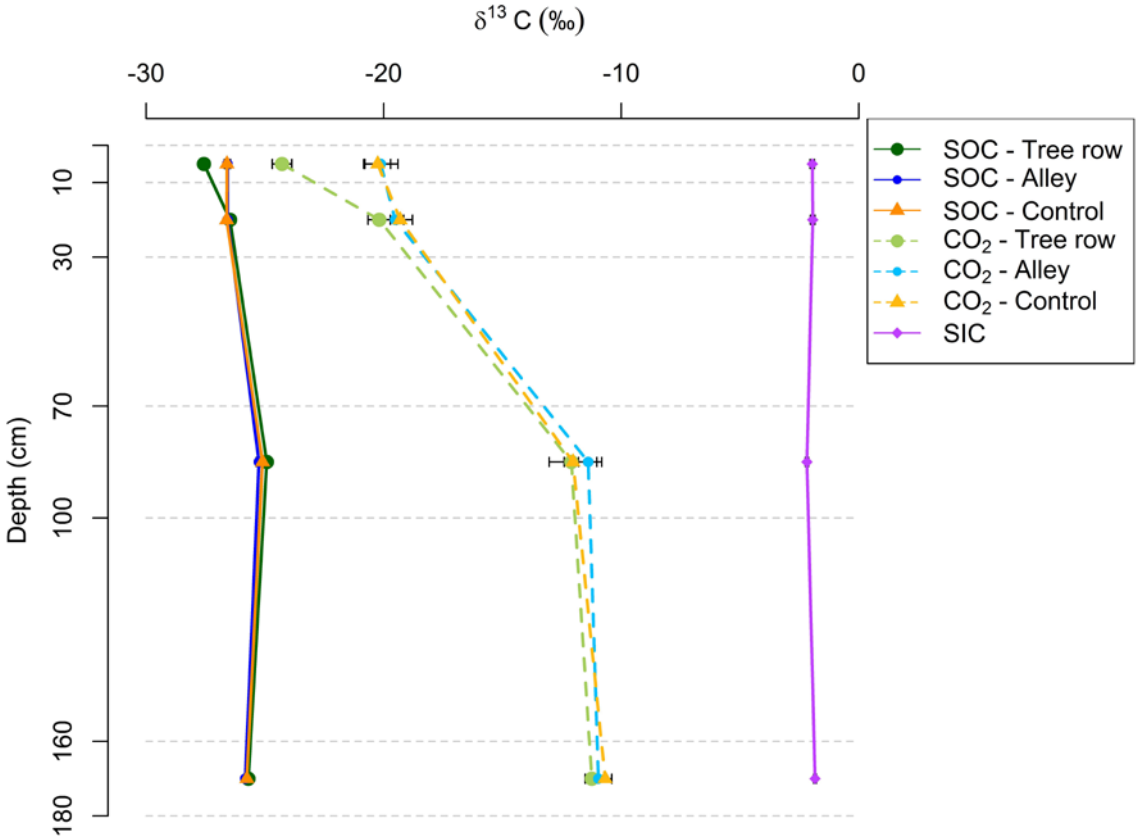

Figure 2 Contribution of soil organic carbon (SOC) and soil inorganic carbon (SIC) derived CO_2 to cumulated CO_2 emissions (µg C-CO_2 g^{-1} soil) during the incubation. C= control plot, A= cropped alley, R: tree row. Error bars are standard errors (N=4). The percentages represent the proportion of CO_2 emissions derived from soil inorganic carbon (SIC).

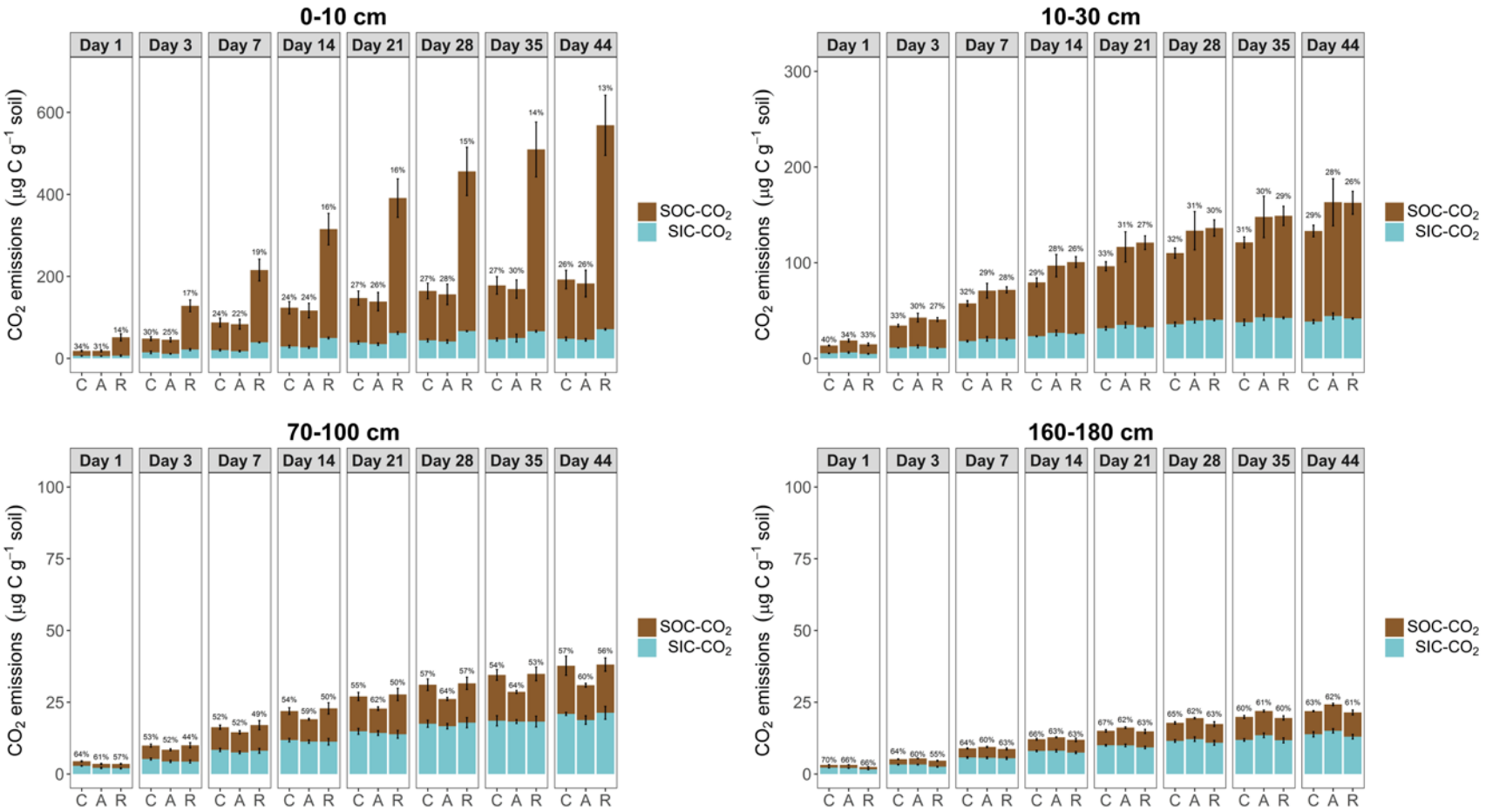

Figure 3 A) Contribution of soil inorganic carbon (SIC) derived CO_2 ($SIC - CO_2$) as a function of SIC content. B) Cumulative $SIC - CO_2$ as a function of cumulative SOC-derived CO_2 ($SOC - CO_2$).

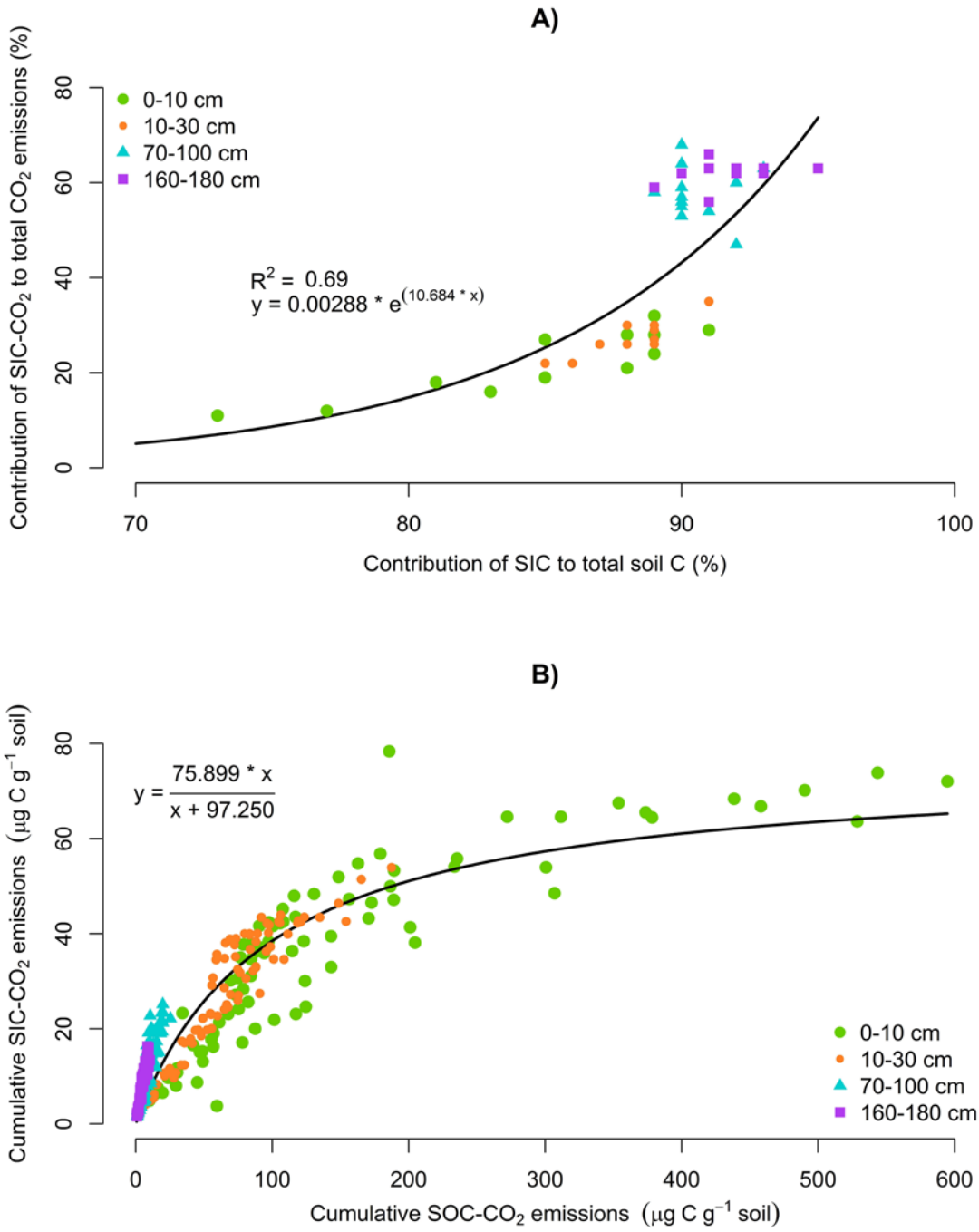

Figure 4 Percentage of initial SOC mineralized during the incubation. Associated errors are standard errors (N=4).